

# Kelvin waves from vortex reconnection in superfluid helium at low temperatures

R. Hänninen

Low Temperature Laboratory, Department of Applied Physics, Aalto University, FI-00076 AALTO, Finland

(Dated: November 10, 2015)

We report on the analysis of the root mean square curvature as a function of the numerical resolution for a single reconnection of two quantized vortex rings in superfluid helium. We find a similar scaling relation as reported in the case of decaying thermal counterflow simulations by L. Kondaurova *et al.* There the scaling was related to the existence of a Kelvin-wave cascade which was suggested to support the L'vov-Nazarenko spectrum. Here we provide an alternative explanation that does not involve the Kelvin-wave cascade but is due to the sharp cusp generated by a reconnection event in a situation where the maximum curvature is limited by the computational resolution. We also suggest a method for identifying the Kelvin spectrum based on the decay of the rms curvature by mutual friction. Our vortex filament simulation calculations show that the spectrum of Kelvin waves after the reconnection is not simply  $n(k) \propto k^{-\eta}$  with constant  $\eta$ . At large scales the spectrum seems to be close to the Vinen prediction with  $\eta = 3$  but becomes steeper at smaller scales.

## I. INTRODUCTION

The decay of quantum turbulence in the limit of zero temperature is one of the key topics that seeks an answer. The Kelvin-wave cascade is one promising way of transferring energy from intervortex distances to smaller scales where the classical Kolmogorov cascade is impossible<sup>1-4</sup>. There the weak nonlinear coupling between different scales of helical distortions (=Kelvin waves) transfers the energy to ever smaller scales until dissipation may become possible, e.g., via phonon emission.

Reconnections and interactions between neighboring vortices are expected to work as a drive that transfers energy from large scales and feeds the Kelvin-wave cascade. At finite temperatures the weak Kelvin cascade is easily suppressed by the mutual friction dissipation<sup>5,6</sup>. In order to understand the decay processes in the zero temperature limit at scales around and smaller than the intervortex distance, we must be able to distinguish between the roles of the Kelvin-wave cascade, the Kelvin waves directly induced by the reconnection events, and the mutual friction dissipation.

Here we concentrate on the Kelvin waves generated by a single reconnection event and investigate whether a Kelvin cascade originates from the reconnection event. We also illustrate how Kelvin waves are damped by mutual friction. Our analysis at zero temperature reveals that soon after a reconnection the vortex becomes filled with Kelvin waves of different scale and that the presence of the shortest scales is limited only by the resolution. However, in accordance with earlier work<sup>7</sup>, the evidence for the existence of the Kelvin cascade remains weak since the observations can be explained by a redistribution of Kelvin waves that are initially “packed inside the reconnection cusp”.

Our paper is organized such that in Sec. II we review the relation between the rms curvature and the Kelvin spectrum. We also take into account the numerical contribution from a single sharp cusp. In Sec. III we consider a straight vortex with Kelvin waves and show how the decay of rms curvature by mutual friction can be used to identify the Kelvin spectrum. We additionally illustrate that the mean curvature can strongly increase without changes in the Kelvin spectrum. In Sec. IV we consider the actual reconnection event and use the results

from previous sections to interpret these results.

## II. MODEL

In superfluid <sup>4</sup>He the vorticity appears in the form of quantized vortices, with circulation quantum  $\kappa = h/m_4 \approx 0.0997$  mm<sup>2</sup>/s, whose core size is of the order of 1 Å. Ignoring compressibility effects, the vortex dynamics can be modeled by using the vortex filament model where the vortices are considered as line defects and the superfluid velocity field is given by the Biot-Savart law. The filament model should be a good model for <sup>4</sup>He-II where the core radius is five to six orders of magnitude below the typical experimental intervortex distance. The model is extensively described, e.g., in Ref. [8]. Numerically the vortex, a three-dimensional curve  $s(\xi, t)$ , where  $\xi$  is the length along the vortex and  $t$  is time, is described by a sequence of points whose motion is here followed by the fourth order Runge-Kutta method. Our numerics is described in more detail in Ref. [7], where we analyzed a similar situation of reconnecting vortex rings but concentrated on the dissipation due to mutual friction.

### A. Kelvin spectrum and rms curvature

The identification of helical Kelvin waves in a vortex tangle is a delicate problem<sup>9</sup>. A proper identification is currently possible only in a few rare cases. In the case of a straight vortex, taken to be along the  $z$  axis, and when the perturbations can be presented as  $w(z) = x(z) + iy(z)$ , the Fourier transformation of  $w(z)$  determines the Kelvin-wave amplitudes  $w_k$ . The Kelvin occupation spectrum is typically defined as

$$n(k) = |w_k|^2 + |w_{-k}|^2, \quad k > 0. \quad (1)$$

One should note that here the  $k$  vector is a one-dimensional vector that defines the wavelength for the Kelvin waves and should not be confused with the amplitude of the three-dimensional  $\mathbf{k}$  vector that is typically used when writing the energy (velocity) spectrum.

To provide a rough measure of the Kelvin waves the distribution of curvature radii can be extracted from a vortex

filament calculation. However, in the general case, to derive the Kelvin spectrum from the curvature spectrum leads to an insolvable inverse problem. In case of a straight vortex, and in the limit of small Kelvin amplitudes, these two spectra are closely related. Unfortunately, the curvature spectrum is typically much too noisy and no proper spectrum can be determined from the curvature data. Therefore, the analysis in Ref. [6] was restricted to the calculation of the root mean square (rms) curvature,  $c_{\text{rms}}$ :

$$c_{\text{rms}}^2 = \frac{1}{L} \int c(\xi)^2 d\xi, \quad (2)$$

where  $c(\xi) = |s''(\xi)|$  is the local curvature at  $\xi$ , and  $L$  is the total vortex length. For small Kelvin amplitudes (more precisely when  $|w'(z)| = |dw/dz| \ll 1$ ) and when the energy is taken to be proportional to the vortex length [localized induction approximation, (LIA)], the energy spectrum  $E(k) \propto k^2 n(k)$  for Kelvin waves with wave number  $k$  can be related to the rms curvature by<sup>6</sup>

$$c_{\text{rms}}^2 \approx \frac{4\pi}{\Lambda \kappa^2} \int_{k_{\min}}^{k_{\max}} k^2 E(k) dk. \quad (3)$$

The term  $\Lambda = \ln(\ell/a_0)$  depends only weakly on the intervortex distance  $\ell$  and on the core radius  $a_0$ . Here the Kelvin spectrum is assumed to be valid from  $k_{\min}$  up to some cutoff scale  $k_{\max}$ , above which the spectrum is suppressed (either due to numerical cutoff or, e.g., by suppression due to mutual friction).

Since the predictions for the Kelvin-wave spectrum vary from  $E(k) \propto 1/k$ , in the case of strong wave turbulence with the Vinen spectrum<sup>10</sup>, to  $E(k) \propto k^{-5/3}$  with the L'vov-Nazarenko spectrum<sup>3</sup>, the rms curvature is not much affected by the scales near  $k_{\min}$ . The dominant contribution originates from scales near  $k_{\max}$  and may therefore be limited by the numerical resolution of the calculation.

The different proposals for Kelvin-wave spectra by Vinen<sup>10</sup> (V), Kozik-Svistunov<sup>2</sup> (KS), and L'vov-Nazarenko<sup>3</sup> (LN) in terms of  $c_{\text{rms}}$  are asymptotically given by<sup>6</sup>

$$\begin{aligned} c_{\text{rms}}^{\text{V}} &= \Phi k_{\max} \\ \ell c_{\text{rms}}^{\text{KS}} &= \Phi (\ell k_{\max})^{4/5} \\ \ell c_{\text{rms}}^{\text{LN}} &= \Phi (\ell k_{\max})^{2/3}. \end{aligned} \quad (4)$$

Generally, when the Kelvin spectrum  $n(k) \propto k^{-\eta}$ , the rms curvature is given by  $c_{\text{rms}} \propto k_{\max}^{(5-\eta)/2}$ . The intervortex spacing  $\ell$  limits the smallest possible  $k$  values, and the term  $\Phi$ , given by

$$\Phi = \sqrt{4\pi E / \Lambda \kappa^2}, \quad E = \int_{k_{\min}}^{k_{\max}} E(k) dk, \quad (5)$$

takes into account the fraction from the total energy  $E$  (per unit length, per unit mass) related to Kelvin waves. Because some numerical factors of the order of unity have been neglected in the above derivation, one should consider  $\Phi$  only as an estimate.

We expect that at low enough temperatures the Kelvin cascade becomes the dominant dissipation mechanism, which at

scales smaller than the intervortex distance transports energy towards the core scales where it can be dissipated. For this to be true, at sufficiently low temperatures the Kelvin-wave cascade causes all our numerically traceable scales to be occupied by Kelvin waves, and the rms curvature becomes determined by the numerical resolution. By repeating simulations with different resolutions one should be able to distinguish between different theories.

This is precisely what was done in Ref. [6] for decaying thermal counterflow, where the scaling for  $c_{\text{rms}}$  weakly supported the explanation in terms of the Kelvin-wave cascade with L'vov-Nazarenko spectrum. The complicated situation was exemplified by the fact that the resolution could only be changed by a factor of 2.7, and no firm proof was obtained.

In the following we consider a simpler case: a single reconnection of two initially linked vortices. In this case we are able to change the resolution by a greater amount. However, first we consider how the rms curvature is affected when a vortex configuration contains a sharp cusp where the curvature may diverge (or at least yield values close to the inverse core size).

## B. Sharp cusp and its effect on rms curvature

As soon as one introduces a reconnection in the filament model one creates a sharp cusp in the vortex configuration. A simplified analytical model for a cusp where the curve has a simple discontinuity in the derivative, being smooth elsewhere, does not necessarily change the rms curvature by a large amount. However, numerically the effect can be much more dramatic. Without additional smoothing, the maximum curvature at the cusp is the inverse resolution, and the region for this curvature peak is of the order of the point separation ( $\Delta \xi_{\text{res}}$ ). Smoothing does not necessarily solve the problem, because it only widens the region and restricts the maximum value.

If we split the integral into the “smooth part”, far from the cusp, and into the region that is strongly affected by the numerics, one obtains that

$$c_{\text{rms}}^2 = \frac{1}{L} \int_{\text{smooth}} c(\xi)^2 d\xi + \frac{b}{L \Delta \xi_{\text{res}}}. \quad (6)$$

Here the numerical factor  $b$  is of the order of unity. It should depend weakly on the numerical details and, e.g., on the initial angle between the vortices before the reconnection. In the limit of high resolution the last term becomes dominant, and the rms curvature due to numerics becomes

$$c_{\text{rms}}^{\text{N}} = \sqrt{\frac{b}{L \Delta \xi_{\text{res}}}} \propto k_{\max}^{1/2}, \quad (7)$$

where  $k_{\max} = 2\pi / \Delta \xi_{\text{res}}$  is determined by the resolution.

If we consider the analytical model (which is based on earlier numerical work) for the vortex shape before the reconnection [11], we get further support for Eq. (7). This estimate for the pre-reconnection vortex shape indicates that the cusp sharpens until the minimum distance reaches the core size (after which the filament model is not valid any more) such that

eventually the region, where the curvature is of the order of the inverse core radius, is also of the order of the core diameter. Simulations with the Gross-Pitaevskii model indicate that the curvature does not increase much from this limit imposed by the core radius and that it also has a similar magnitude after the reconnection<sup>12</sup>. Therefore, Eq. (7) should originate already from the prereconnection dynamics where  $k_{\max}$  is given by the core size.

Even if the cusp contribution to  $c_{\text{rms}}$  grows slower with  $k_{\max}$  than the cascade predictions in Eqs. (4), it may give the dominant contribution when the Kelvin amplitudes are small ( $\Phi \ll 1$ ) and when the resolution is not high enough, as shown below. Its contribution also increases with increasing number of reconnections.

In addition to the rms curvature, we also use the mean curvature  $c_{\text{ave}}$  in our analysis:

$$c_{\text{ave}} = \frac{1}{L} \int c(\xi) d\xi. \quad (8)$$

Based on similar arguments as used for the rms curvature in Eq. (6), the contribution from the cusp region should result in a constant contribution that does not increase as the resolution is improved, i.e.,

$$c_{\text{ave}} = \frac{1}{L} \int_{\text{smooth}} c(\xi) d\xi + \frac{\tilde{b}}{L}, \quad (9)$$

where  $\tilde{b}$  is another constant of the order of unity. Because  $c_{\text{ave}}$  is sensitive to the phases of the Kelvin waves it cannot be directly related to the Kelvin spectrum.

### III. KELVIN WAVES ON A STRAIGHT VORTEX

In order to better understand simulations where Kelvin waves are produced by a single reconnection event, we first consider two simplified sets of simulations for a straight vortex where the determination of the Kelvin spectrum is less challenging. These calculations model the time development *after* the reconnection. In both cases we occupy the straight vortex, taken to be along the  $z$  axis, with a known Kelvin spectrum parametrized as

$$n(m) = |w_m|^2 + |w_{-m}|^2 = A^2 m^{-\eta}, \quad m = 1, 2, 3, \dots \quad (10)$$

Here  $A$  determines the amplitude of the Kelvin spectrum, and the  $w_m$ 's can be obtained by Fourier transformation of  $w(z)$ , provided that the configuration remains single valued. At the instant when the single valuedness breaks,  $|dw/dz|$  diverges. The  $k$  vector  $k = 2\pi m/L_z$  is given by the mode number  $m$  and period  $L_z$ . In all these calculations we have fixed the reactive mutual friction parameter  $\alpha' = 0$ .

We can make an analytical approximation for the time development of  $c_{\text{rms}}$  if we assume that the Kelvin-wave cascade is absent such that every Kelvin mode decays exponentially as  $w_m(t) = w_m(0)e^{-t/\tau_{\alpha m}}$ , where  $\tau_{\alpha m} = \tau_{11}/(\alpha m^2)$ . With  $\tau_{11}$  we denote the decay time for mode  $m = 1$  when  $\alpha = 1$ . We neglect the weak logarithmic  $m$  dependence in  $\tau_{\alpha m}$ . By assuming that initially  $w_m(0)$  has a spectrum defined by Eq. (10),

we obtain by using the small amplitude estimation, where  $c(\xi) \approx |w''(z)|$  and  $d\xi \approx dz$ , that

$$c_{\text{rms}}^2(t) = \frac{(2\pi)^4 A^2}{LL_z^3} \sum_{m>0} m^{4-\eta} e^{-2\alpha m^2 t/\tau_{11}}. \quad (11)$$

Here the vortex length  $L = L(t) \approx L_z$  depends on time only weakly. By taking  $k_{\max} \rightarrow \infty$  and approximating the sum with an integral we obtain, for  $\eta < 5$ , the asymptotic decay curve for the rms curvature as

$$c_{\text{rms}}(t) = \frac{(2\pi)^2 A}{L_z \sqrt{2LL_z}} \sqrt{\Gamma\left(\frac{5-\eta}{2}\right)} \left(\frac{2\alpha t}{\tau_{11}}\right)^{\frac{1}{4}(\eta-5)}, \quad (12)$$

where  $\Gamma(a)$  is the gamma function. If for brevity we write  $c_{\text{rms}} = D(\alpha t)^{-\beta}$ , then the decay exponent  $\beta = (5 - \eta)/4$  is simply given by the Kelvin spectrum. Therefore, if the Kelvin-wave cascade is negligible during the time window when the decay occurs, the above law can be used to identify the initial Kelvin spectrum, as shown below.

If one wants to improve the above approximation, Eq. (12), at small times by taking into account the finite resolution, one should only replace the gamma function with the incomplete (lower) gamma function  $\gamma(a, x)$  as  $\Gamma((5 - \eta)/2) \rightarrow \gamma((5 - \eta)/2, 2\alpha t m_{\max}^2/\tau_{11})$ . Here  $m_{\max}$  is the largest Kelvin mode present, which is limited by the resolution. At large times Eq. (12) fails when only a few lowest modes are present (dominant). Eventually the decay is simply given by the exponential decay of modes  $m = \pm 1$ .

#### A. Decay of rms curvature via mutual friction

In our first sample case, we use different Kelvin spectra with different amplitudes, and observe how the rms curvature decays by the dissipative mutual friction  $\alpha(T)$ . We have additionally assumed that initially the phases of the Kelvin waves are random and that  $|w_m| = |w_{-m}|$ . Figure 1 summarizes our results in case of  $A = 0.01L_z$  and  $\alpha = 0.1$ . The number of points used is 1024 and  $L_z = 1$  mm.

By repeating the calculations with different values of  $\alpha$ , we observe that the decay curve  $c_{\text{rms}} = D(\alpha t)^{-\beta}$  is universal, as predicted by Eq. (12), and the terms  $D$  and  $\beta$  are not essentially affected by the mutual friction parameter  $\alpha$ . Also, the exponent  $\beta$  is almost solely given by the Kelvin spectrum exponent  $\eta$ , as shown by the lower inset of Fig. 1, where we have used a time window  $10^{-5} \text{ s} < \alpha t < 10^{-3} \text{ s}$  for the fit. The lower (red) curve is calculated for a relatively large amplitude  $A/L_z = 0.1$ , where the energy related to Kelvin waves is of similar order as the energy related to the straight vortex. The upper (blue) curve is appropriate for the small amplitude limit  $A/L_z = 0.001$ . Further expansion of the amplitude window does not essentially change the results.

The amplitude  $D$  is mainly determined by the Kelvin amplitude  $A$ . This is illustrated in the upper inset of Fig. 1 using the L'vov-Nazarenko spectrum. The small time behavior, which originates from the smallest scales, is sensitive to the resolution and is consistent with the saturation if the full Eq. (11), or

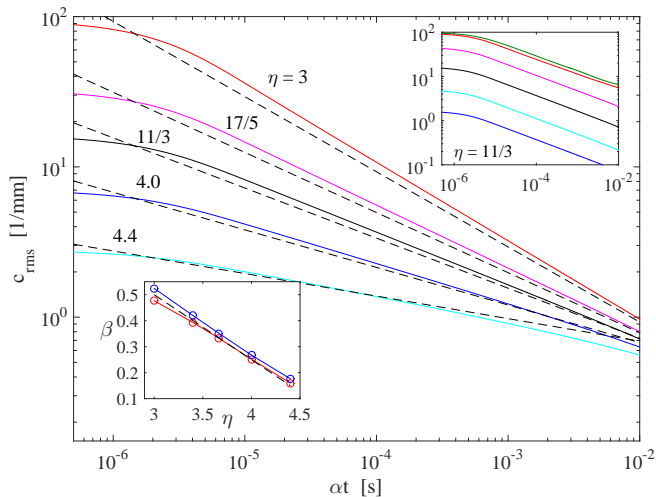


FIG. 1. (Color online) Decay of  $c_{\text{rms}}$  for different initial Kelvin spectra on a straight vortex with periodic boundary conditions and period  $L_z = 1$  mm. The number of points is 1024 and  $\alpha = 0.1$ . In the *main panel* the amplitude is  $A/L_z = 0.01$ , see Eq. (10). The different spectra are from top to bottom defined by  $\eta = 3.0$  (red, Vinen), 3.4 (magenta, Kozik-Svistunov), 3.666... (black, L'vov-Nazarenko), 4.0 (blue), and 4.4 (cyan), respectively. The dashed lines are from the analytical model, Eq. (12). The *upper inset* shows the  $c_{\text{rms}}$  for the LN spectrum but for different amplitudes: from top to bottom  $A/L_z = 0.3, 0.1, 0.03, 0.01, 0.003, \text{ and } 0.001$ , respectively. The *lower inset* relates the decay exponent  $\beta$  in  $c_{\text{rms}} \propto t^{-\beta}$  to the exponent  $\eta$  in the Kelvin spectrum of Eq. (10). The upper (blue) curve is for small amplitudes with  $A/L_z = 0.001$ , and the lower (red) curve is for rather large amplitudes with  $A/L_z = 0.1$ . The thin dashed line is the exponent appearing in the analytical result [see Eq. (12)].

the approximation described below Eq. (12), is used. Therefore, the power law can be validated also at early times simply by improving the resolution.

If we use the value  $\tau_{11} \approx 0.22$  s from the calculations where only the mode  $m = 1$  is present and approximate that  $L \approx L_z$ , we obtain nice quantitative agreement with Eq. (12), not only for the exponent, but also for the absolute amplitude. This is illustrated in Fig. 1 with the dashed lines. The general tendency for deviations upwards from the theory prediction, Eq. (12), originates from the omitted logarithmic  $\ln(m)$  dependence in  $\tau_{m\alpha}$ . The deviations downwards at large times (which is visible in Fig. 1 for  $\eta = 4.4$  and 4.0) can be understood to originate from the finite period which results in that eventually only the longest Kelvin waves with wavelength equal to  $L_z$  persist and decay exponentially. Equation (11) models this limit accurately.

The decay curve for  $c_{\text{rms}}$  is not sensitive to the initial phases of the Kelvin waves, as expected from the derivation where the phases are not present. We have also numerically checked that on the scale of Fig. 1 one cannot resolve two different decay curves with different initial sets of random phases.

If we analyze the decay of the different Kelvin modes in Fig. 1, we may verify that the different Kelvin modes actually rather well exhibit exponential decay where the time scale is determined by  $\alpha$  and  $k$ . There are additionally fluctuations

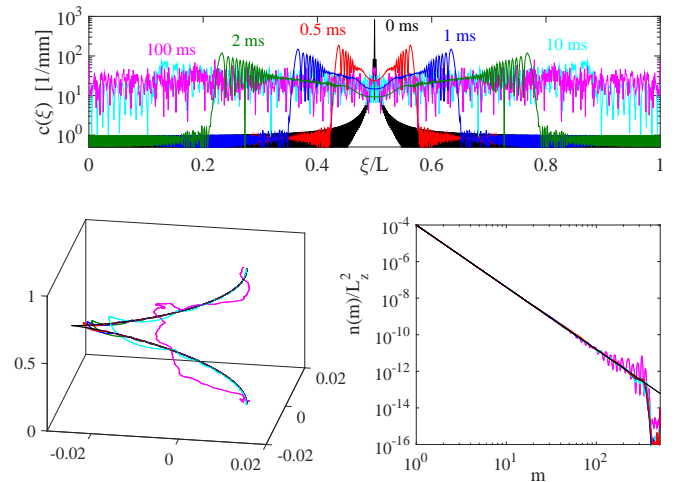


FIG. 2. (Color online) Time development of the “test-cusp” vortex at  $T = 0$  that initially hosts the Kozik-Svistunov spectrum. The *upper panel* illustrates the time development of the local curvature at times 0 (black), 0.5 (red), 1 (blue), 2 (green), 10 (cyan), and 100 ms (magenta). The *lower left panel* shows the corresponding vortex configurations, and the *lower right panel* contains the Kelvin spectra where  $k = 2\pi m/L_z$  is given by the mode number  $m$ .

that are due to interactions between different modes. Also, the decay only continues for about four to five orders of magnitude, which is likely due to numerics. We have not checked the situation for very small  $\alpha$  values because it requires a large enough time window. This would be important if one seeks the Kelvin cascade, but if the intention is to determine the initial Kelvin spectrum one is not required to use extremely small values of mutual friction. Actually, it is much more convenient to use a large enough  $\alpha$  in order to minimize the effect from the cascade during the decay of  $c_{\text{rms}}$ .

Therefore, if the characteristic curvatures are much larger than the inverse of the intervortex distance  $1/\ell$ , the decay of  $c_{\text{rms}}$  should provide a potential way to identify the Kelvin spectrum, perhaps also in more complicated tangles.

## B. Cusp built by Kelvin waves

In our second example case we illustrate how a cusp, where the curvature is strongly peaked, can be built on a straight vortex using a Kelvin spectrum defined by Eq. (10). We then follow its dynamics both at  $T = 0$  and  $T > 0$ .

The phases of the Kelvin waves are typically considered to be random, which results in a wiggly looking vortex. However, by specially organizing the phases one may generate a vortex that is otherwise smooth but contains a single cusp (per period). In Fig. 2 we have built a “test-cusp” by setting the same constant phase for all the Kelvin waves using the Kozik-Svistunov spectrum. The period is  $L_z = 1$  mm, and the number of points is 1024. All the Kelvin waves have rather small amplitude  $A/L_z = 0.01$ , but since the phases are the same,  $|w'(z)| \approx 0.5$  near the cusp. Therefore, the theory predictions made in Sec. II are not necessarily valid, e.g., the rms curva-

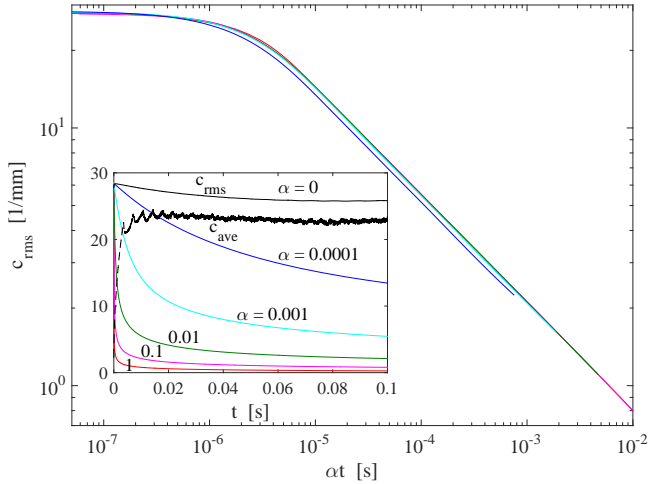


FIG. 3. (Color online) Decay of the rms curvature when the initial configuration is a specially arranged sharp cusp with Kozik-Svistunov spectrum, see Fig. 2. The different curves correspond to different values of mutual friction:  $\alpha = 0.0001$  (blue),  $0.001$  (cyan),  $0.01$  (green),  $0.1$  (magenta), and  $1$  (red). The *inset* shows the time development for  $c_{\text{rms}}$ , and in addition at  $\alpha = 0$  (black) both for  $c_{\text{rms}}$  (solid) and  $c_{\text{ave}}$  (dashed), plotted on a linear time scale.

ture grows slower than the  $c_{\text{rms}} \propto k_{\text{max}}^{4/5}$  prediction.

The upper panel of Fig. 2 shows the time development of the local curvature at  $T = 0$ . It seems that with increasing time more small scale structure is developing because Kelvin waves spread from the cusp and eventually fill the whole vortex. However, if one investigates the corresponding Kelvin spectra, shown in the lower right panel of Fig. 2, the amount of Kelvin waves ( $= \int_{k_{\text{min}}}^{k_{\text{max}}} n(k) dk$ ) is not essentially changed because the spectrum is still the same (initial) Kozik-Svistunov spectrum. Deformations occur only near the resolution limit, where the numerical errors are largest.

As the cusp relaxes, the phases of the Kelvin waves randomize because all the Kelvin waves have different propagation velocity along, and different rotation velocity around, the  $z$  axis. This results in that the mean curvature, which initially is much smaller than the rms curvature, grows and soon has a similar value as  $c_{\text{rms}}$ . This is illustrated in the inset of Fig. 3, where we have analyzed the decay of the rms curvature by mutual friction, for different values of  $\alpha$ . The main panel shows that the decay follows the universal power law with exponent  $\beta = 0.4$ , derived above for the KS spectrum (Fig. 1).

## IV. RECONNECTION OF TWO LINKED VORTEX RINGS

### A. Numerical setup

We consider two vortex rings with radius  $R = 1$  mm, initially linked and oriented perpendicular to each other. The initial distance between the two vortices is  $0.1R$ , causing that at  $T = 0$  they will reconnect approximately at  $1.696$  s. For dynamics, see Ref. [7]. Our reconnection method is rather standard: We reconnect the vortex segments when the mini-

um distance becomes smaller than  $0.8\Delta\xi_{\text{min}}$ , where  $\Delta\xi_{\text{min}}$  is the minimum point separation tolerated. The maximum point separation allowed is  $\Delta\xi_{\text{max}} = 2\Delta\xi_{\text{min}}$ . Additionally, we require that the vortex length must decrease, which approximately means that the reconnection event is dissipative.

The time resolution is chosen such that our numerical time step is kept smaller than the time scale related to the smallest resolvable Kelvin waves. This implies that our time step  $\Delta t \propto (\Delta\xi_{\text{min}})^2$ , resulting in that the better the spatial resolution, the more difficult it becomes to cover the same overall time window as in the lowest resolution run. Another numerical challenge is caused by the fact that the computational work per one time step grows as  $N^2 \propto (1/\Delta\xi_{\text{min}})^2$ , where  $N$  is the number of points used to describe the vortex.

### B. Finite mutual friction

Before concentrating on the zero temperature limit we show how finite mutual friction affects the vortex dynamics and how it damps the Kelvin waves generated by the reconnection cusp. In Fig. 4 we have plotted the rms curvature for one particular resolution, defined by  $\Delta\xi_{\text{min}} = 0.0025$  mm, for seven different values of the mutual friction parameter  $\alpha$  (in all cases  $\alpha' = 0$ ).

For  $\alpha \sim 1$  the instant of reconnection depends essentially on  $\alpha$  because the vortex rings shrink more and therefore they also move faster. The relaxation rate for  $c_{\text{rms}}$  is strongly affected by the mutual friction. However, one may notice that the peak value, just after the reconnection, is not substantially affected by  $\alpha$ . The changes are mainly due to the numerical algorithm used for the reconnection. This causes that the distance between the neighboring vortices is not exactly the same when the reconnection is made, and therefore the sharpness/angle of the cusp may slightly vary.

If we compare these results with the model system, Sec. III A, we may conclude that the results are consistent with the idea that the amplitude of the Kelvin wave decays exponentially with time scale  $\tau \propto 1/(\alpha k^2)$ . These Kelvin waves are generated by the reconnection, and the  $\alpha$  scaling shown in the main panel of Fig. 4 is consistent with the idea that the Kelvin-wave cascade is absent. If, at low enough temperatures, the Kelvin cascade would become important (compared with mutual friction), then the same scaling would not work anymore because the cascade should continuously generate new small scale Kelvin waves and  $c_{\text{rms}}$  should decay slower (or perhaps even grow). Note that a similar scaling relation is obtained and plotted for the mutual friction dissipation power in Fig. 5 of Ref. [7].

The absence of the Kelvin cascade is additionally supported by the decay curve, plotted with the black dash-dotted line in Fig. 4. Here the decay is calculated using  $\alpha = 0.01$ , but the initial configuration is taken from the zero temperature calculations with  $\alpha = 0$  one second after the reconnection. Since the decay follows exactly the same curve as the standard  $\alpha = 0.01$  case, the two spectra are likely the same. Therefore, even during that one second period, which corresponds to the Kelvin period with a wavelength of the order of  $R = 1$  mm, the

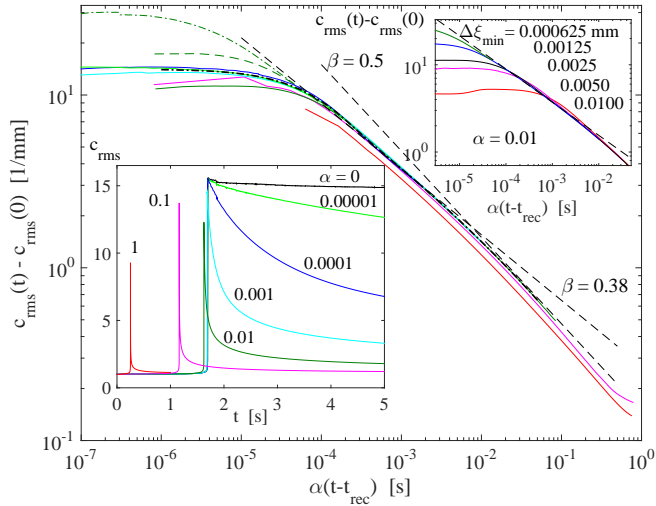


FIG. 4. (Color online) Time development of the rms curvature for different values of the mutual friction parameter  $\alpha$  (and  $\alpha' = 0$ ). In the *main figure* time is measured from the reconnection instant and scaled by  $\alpha$ , and on the vertical axis the initial curvature  $c_{\text{rms}}(0) = 1/R$  is subtracted from the data. Different colors are used for  $\alpha = 1$  (red), 0.1 (magenta), 0.01 (green), 0.001 (cyan), 0.0001 (blue), and 0.00001 (light green), respectively. The corresponding maximum times simulated are 1, 9, 10, 12, 20, and 30 s, respectively. The black dash-dotted curve is for  $\alpha = 0.01$  where the initial configuration is taken from  $T = 0$  simulations, 1 s after the reconnection, and the time (which covers a time window of 5 s) is measured from this instant. The curves are calculated with a resolution of  $\Delta\xi_{\text{min}} = 0.0025$  mm, while for  $\alpha = 0.01$  results with  $\Delta\xi_{\text{min}} = 0.00125$  mm (dashed, green) and 0.000625 mm (dash-dotted, green) are also shown. The power-law behavior is illustrated by plotting the  $c_{\text{rms}} \propto (\alpha t)^{-\beta}$  asymptotics with  $\beta = 0.5$  and  $0.38$  (dashed) that correspond to  $\eta = 3$  and  $3.48$ , respectively. In the *lower inset* linear scales are used without any scaling. The color coding is the same as in the main figure. The case  $\alpha = 0$  is additionally shown by the black curve. The *upper inset* is for  $\alpha = 0.01$  with five different resolutions indicated on the plot, together with the  $\beta = 0.38$  asymptotic (dashed line).

interactions between different Kelvin modes have not altered the spectrum which was directly generated by the reconnection at  $T = 0$ .

The observed decay exponent in our reconnection calculation (see Fig. 4) at late times (large scales) is close to  $\beta = 0.5$ , which corresponds to the Vinen spectrum ( $\eta = 3$ ) for the Kelvin waves. This has been suggested, e.g., in Ref. [10]. At early times, which correspond to small scales, the decay slope is slower, and one obtains a reasonable fit using  $\beta = 0.38$ . Using the analytical model in Eq. (12), this corresponds to  $\eta = 3.48$ . In the upper inset the decay behavior with  $\alpha = 0.01$  is illustrated using five different resolutions. The two highest resolutions are also included in the main panel of Fig. 4. The slope at early times is close to the predictions by Kozik-Svistunov<sup>2</sup> with  $\eta = 3.4$ , but here the spectrum is generated directly by the reconnection, without the need for a cascade.

The difficulty in finding a good fit with fixed  $\beta$ , that would cover the whole time window for the decay of  $c_{\text{rms}}$ , may indicate that the Kelvin spectrum is not necessarily given by

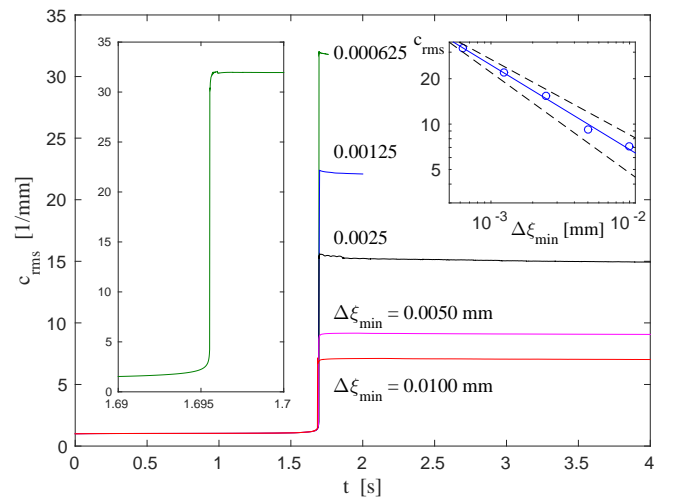


FIG. 5. (Color online) Time development of the rms curvature at  $T = 0$  for five different resolutions where the point separation is kept between  $\Delta\xi_{\text{min}} \dots 2\Delta\xi_{\text{min}}$ . For the two highest resolution runs, times well before the reconnection were omitted and the calculations were continued using the configuration from the run with one step lower resolution where the configuration was still smooth. The *left inset* shows the detailed behavior near the reconnection event when  $\Delta\xi_{\text{min}} = 0.000625$  mm. The *right inset* shows the scaling relation for the root mean square curvature after the reconnection as a function of resolution plus the fit  $c_{\text{rms}} \propto \Delta\xi_{\text{min}}^{-0.56}$  (solid line) and the predictions from the L'vov-Nazarenko spectrum (lower dashed) and from the single cusp model (upper dashed).

Eq. (10) with constant  $\eta$ . It seems that the smaller the scale the bigger is  $\eta$ . This is consistent with the idea suggested by Nazarenko in Ref. [13], where he argued that the reconnection drives not only length scales near the intervortex distance but also smaller scales. Therefore, the spectrum excited by the reconnection would depend on scales. Now these simulations illustrate that the spectrum is not simply  $n(k) \propto k^{-4}$  that can be associated with a sharp bend.

### C. Zero temperature results

In the zero temperature limit, where the mutual friction decay time for the single Kelvin wave diverges,  $c_{\text{rms}}$  does not essentially decay after the reconnection kink has appeared but remains sensitive to the numerical resolution. Figure 5 illustrates the time development of the calculated rms curvature when the resolution is changed by a factor of 16 while  $\alpha = 0$ . The inset illustrates that the curvature starts to increase already before the reconnection due to nonlocal interactions. This tends to strongly deform the vortex shape near the reconnection point. The noticeable jump at the instant of reconnection appears due to the appearance of the sharp cusp which is sharpest immediately after the numerical reconnection process. Therefore, very locally the curvatures reach the values determined by the resolution.

After the reconnection the rms curvature may slightly increase and later decrease, but very soon after the reconnection

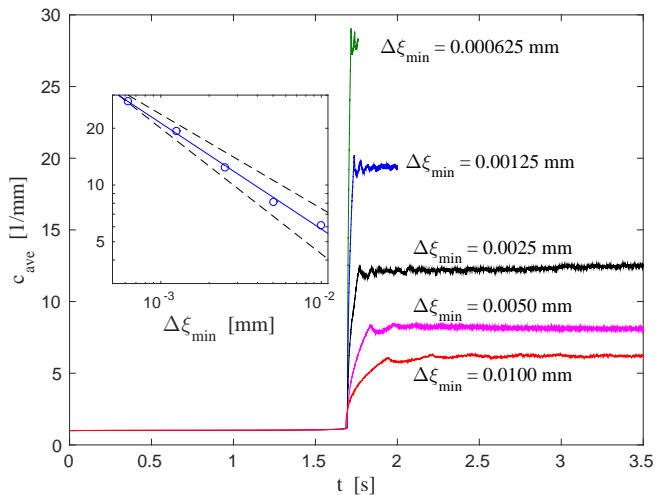


FIG. 6. (Color online) Time development of the mean curvature for the same five different resolutions which were used to plot the rms curvature in Fig. 5. The *inset* shows a similar scaling relation as that for  $c_{\text{rms}}$ . The solid line is a fit,  $c_{\text{rms}} \propto \Delta\xi_{\text{min}}^{-0.56}$ , to the data points, and the dashed lines are again the predictions from the L'vov-Nazarenko spectrum (lower dashed) and from the single cusp model (upper dashed).

$c_{\text{rms}}$  remains constant. This is consistent with the LIA approximation where  $c_{\text{rms}}$  is one of the several constants of motion and where cascade formation is not allowed. We have continued our  $\Delta\xi_{\text{min}} = 0.005$  mm calculation up to 100 s, and in addition to the small  $\sim 1\%$  decay of  $c_{\text{rms}}$  during this time; it possesses oscillations with amplitude  $\sim 1\%$  and period  $\sim 20$  s. This makes it difficult to say accurately from shorter simulation runs whether the curvature actually decays, or whether the initial smaller decay is just part of these oscillations.

If we plot the approximately constant value of  $c_{\text{rms}}$  after the reconnection as a function of the resolution one may observe a scaling relation, similar to the predictions above. This is shown in the inset of Fig. 5. The fitted exponent is 0.56, which is closer to the prediction for a simple cusp than the one originating from the Kelvin cascade with L'vov-Nazarenko spectrum. If we want to relate the exponent to a particular spectrum, the value corresponds to  $\eta = 3.88$ . Within the cusp model, if we use the minimum point separation instead of  $\Delta\xi_{\text{res}}$  in Eq. (7), we obtain  $b \approx 7$ . This is consistent with our prediction (note that our configuration has two cusps).

In Fig. 6 we have plotted the time development of the mean curvature. One may observe that the large sudden jump, present for the rms curvature, is now missing at the instant of reconnection. Rather, the mean curvature starts to increase after the reconnection and finally stabilizes to a value very similar to  $c_{\text{rms}}$ . Therefore, also the  $c_{\text{ave}}$  satisfies a similar scaling relation as  $c_{\text{rms}}$ .

The time scale for reaching the final value in Fig. 6 is determined by the resolution, and the increase in  $c_{\text{ave}}$  appears because small scale Kelvin waves travel from the reconnection site and quickly fill the whole vortex. The better the resolution, the faster the smallest Kelvin waves travel, and therefore the time scale for reaching the “steady-state” value for  $c_{\text{ave}}$  is

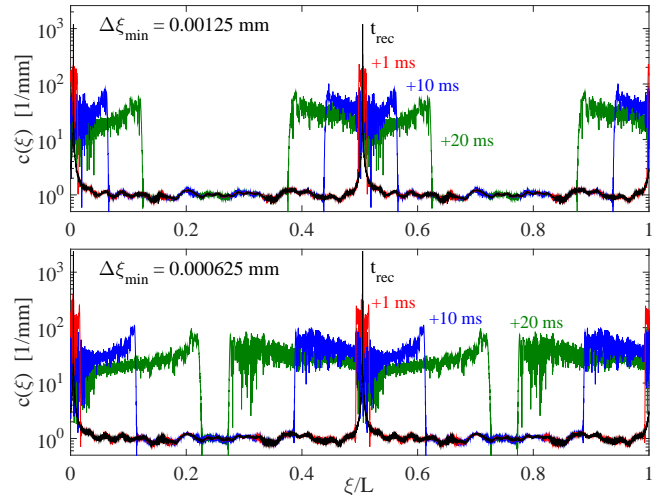


FIG. 7. (Color online) Time development of the local curvature at  $T = 0$  along the vortex after the reconnection of two rings. The reconnection results in two strong peaks at locations  $\xi \approx 0$  and  $\xi \approx 0.5L$ . The *upper panel* is for the resolution  $\Delta\xi_{\text{min}} = 0.00125$  mm, and the *lower panel* is for twice better resolution,  $\Delta\xi_{\text{min}} = 0.000625$  mm. The black curve is immediately after the reconnection, and other curves are 1 ms (red), 10 ms (blue), and 20 ms (green) after the reconnection. Note the logarithmic vertical axis and that the maximum speed of the spreading Kelvin waves is limited/defined by the resolution.

directly proportional to the point separation used. This redistribution of the Kelvin waves is illustrated in Fig. 7, where the local curvatures are plotted at different times.

One might argue that the increase in  $c_{\text{ave}}$  proves the existence of the Kelvin cascade because it seems that more small scale structure appears. This is possible, but it is not the only possible explanation. First, scaling relations similar to those in Eq. (4) cannot be easily derived for  $c_{\text{ave}}$  from the Kelvin-wave spectrum. Second, the mean curvature can be strongly increased by simply adjusting the phases of the Kelvin waves without changing the Kelvin spectrum, i.e., without changing the amplitudes of small scale Kelvin waves. This is illustrated by our “test-cusp” in Sec. III B, see Fig. 3. In the small amplitude limit, which is not necessarily a proper assumption for a cusp, the phases of Kelvin waves do not change  $c_{\text{rms}}$ , as shown by Eq. (3). Instead, the increase in the average curvature  $c_{\text{ave}}$  in Fig. 6 after the reconnection appears as the phases “randomize” from their initial values at the instant of reconnection.

The above phase randomization can be understood by considering a vortex with a shape of a triangle wave whose mean curvature is zero. It has a Fourier representation with only odd indices  $k = 1, 3, 5, \dots$  whose amplitudes go like  $w_k \propto 1/k^2$ , corresponding to the Kelvin spectrum  $E(k) \propto 1/k^2$  (equal to the Kelvin occupation spectrum  $n_k \propto |w_k|^2 \propto 1/k^4$ ), not far from the LN spectrum. The Kelvin waves present in this kind of configuration have a different frequency around the “average vortex direction” (the direction which is realized when the amplitude of the triangle wave goes to zero) and different propagation velocities. Therefore, the vortex has soon a

rather different shape with a mean curvature much larger than initially. This does not require any cascade.

One may still wonder why the Kelvin spectrum, determined from the decay curve at small scales where  $\eta \approx 3.5$ , does not show up in the scaling relation for  $c_{\text{rms}}$ , which is close to the cusp model (or alternatively would correspond to Kelvin spectrum with  $\eta \approx 3.9$ ). One possible reason for this difference might be that the amplitude of the Kelvin spectrum is too small, and therefore the cusp contribution still dominates when calculating the rms curvature. If we compare Eqs. (4) and (7) we find, by setting  $k_{\text{max}} = \pi/\Delta\xi_{\text{min}}$ , that these estimates give the same value for  $c_{\text{rms}}$  when

$$\Phi = \pi^{-\gamma} \sqrt{b/L} \ell^{1-\gamma} \Delta\xi_{\text{min}}^{\gamma-1/2}, \quad (13)$$

where  $\gamma = (5 - \eta)/2$  is the general exponent in Eq. (4) for  $k_{\text{max}}$ . We may crudely approximate that the energy associated to Kelvin waves is related to the increase in vortex length, which is around 1% in our example case<sup>14</sup>, and therefore  $\Phi \approx 0.1$ . If we use  $b = 7$  from our fit,  $L \approx 4\pi R$ , and additionally approximate that  $\ell = R = 1$  mm, we obtain that the small scale spectrum with  $\eta \approx 3.5$ , which dominates the calculation of rms curvature, should be visible in the scaling relation for  $c_{\text{rms}}$  if the resolution is better than  $\Delta\xi_{\text{min}} = 0.01$  mm. Our resolution is almost always better than this. Because we only see the steeper spectrum in the  $c_{\text{rms}}$  scaling (Fig. 5), the Kelvin spectrum near the resolution might be steeper than  $\eta=3.5$ , or alternative because the assumption  $|w'(z)| \ll 1$  is likely not valid, the rms curvature grows slower than predicted by Eqs. (4). Also, the above approximation is rather sensitive to the value of  $\Phi$ . By using  $\Phi = 0.05$  the critical resolution increases to  $\Delta\xi_{\text{min}} = 0.0006$  mm, which is the best resolution used. Now, the cusp contribution should always dominate.

## V. DISCUSSION

In more complicated tangles, where vortices experience a large number of reconnections, the rms curvature can remain high only if the average time between successive reconnections is smaller than the time scale for mutual friction damping. This implies that the temperature must be low enough, as observed in simulations depicting decaying counterflow turbulence<sup>6</sup>. By considering only a single reconnection event we are still far from explaining the dissipation in more complicated tangles where reconnections occur continually. The future question might be to explain what happens to existing Kelvin waves when a new reconnection occurs. Strong local stretching caused by a reconnection is likely to damp the pre-existing Kelvin waves near the reconnection site.

Our method of determining the Kelvin spectrum from the decay of  $c_{\text{rms}}$ , i.e., obtaining  $\eta$  from the fitted value of the decay exponent  $\beta$ , could also be applied to more complicated vortex tangles. If one needs to avoid reconnections one could apply the method separately for each vortex. One may use rather high values of mutual friction and simulate only over a short time window to obtain the scaling law. Actually, with large enough mutual friction the effects from the cascade are

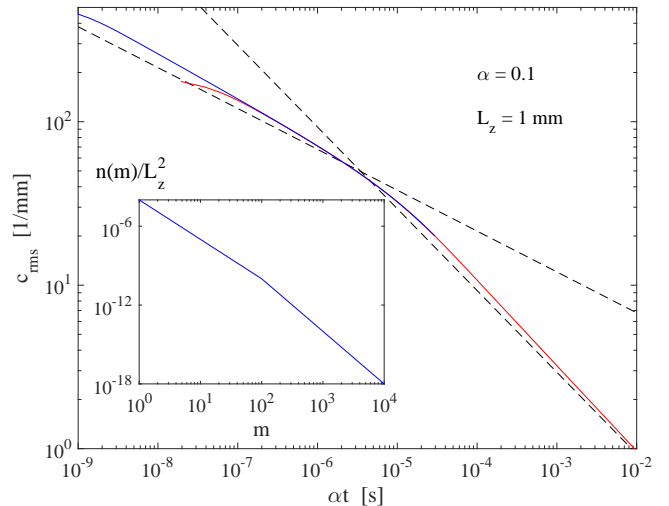


FIG. 8. (Color online) Decay of the rms curvature in the case of a straight vortex when  $\alpha = 0.1$  and  $L_z = 1$  mm. The initial Kelvin spectrum, shown in the inset, is the Vinen spectrum with  $\eta = 3$  and  $A = 0.01L_z$  at low  $k$ 's, while at high  $k$ 's the spectrum is parametrized by  $\eta = 4$  and  $A = 0.1L_z$ . The early time behavior (blue curve) is determined using 65536 points on the vortex, while 8192 points is used to obtain the late time asymptotic (red curve). The dashed lines are the analytical results, Eq. (12), corresponding to both spectra.

minimized and one obtains more accurately the Kelvin spectrum which describes the initial state of the vortex. However, with large  $\alpha$  we cannot immediately tell whether the spectrum is due to a cascade or due to other means like excitations from reconnections. If the cascade should become important at low enough temperatures, it should then result in the decay law of Eq. (12) not being satisfied anymore. This change can be verified by repeating the decay analysis at these lower temperatures.

A nonconstant decay exponent  $\beta$  is likely to originate from a Kelvin spectrum where  $\eta$  is not universal. This is supported by the simulations, similar to the ones presented in Sec. III A, where we have occupied a straight vortex by using the Vinen spectrum at low  $k$ 's ( $m < 100$ ) with amplitude  $A/L_z = 0.01$ , while using a steeper spectrum with  $\eta = 4$  at high  $k$ 's with  $A/L_z = 0.1$ , such that the spectrum remains continuous. The resulting decay curve has a wide crossover region where  $\beta$  changes but both asymptotics follow nicely the theory prediction, Eq. (12). This is illustrated in Fig. 8.

The initial approximately constant value of the rms curvature, seen, e.g., at small values of  $\alpha t$  in Fig. 1, illustrates that the numerical resolution determines when the simulation is numerically in the zero temperature limit. In this limit even the smallest resolvable scales are not smoothed out by mutual friction. From the decay of the smallest scale Kelvin waves one may derive that if  $\alpha\Delta t \ll (\Delta\xi_{\text{res}})^2/\kappa$  then the effects from mutual friction are negligible within times of order  $\Delta t$ . This is consistent with the observations by Kondaurova *et al.*<sup>6</sup> where their simulations at  $T \lesssim 0.5$  K are essentially the same as those conducted at  $T = 0$ .

The presence of the Kelvin-wave cascade in simulations has



been a controversial topic. The concern concentrates around the computational resolution required to resolve the excitations at short length scales in the zero-temperature limit. In Ref. [15] Kivotides *et al.* study the reconnection of four rings in  $T = 0$  simulations and report excitation of Kelvin waves on different scales, including the appearance of a cascade. The later conclusion is not in agreement with our findings. However, in the simulations of Ref. [15] the extremely crinkled shape of the vortex after the reconnection differs from simulations conducted later<sup>7,16</sup> where more effort has been spent on the numerical stability and conservation of energy. See also Ref. [9] for numerical challenges that appear when Kelvin waves are being identified.

## VI. CONCLUSIONS

Based on vortex filament simulations for a single reconnection event in superfluid helium, we have developed an explanation for the scaling relation seen for the rms curvature as a function of the numerical resolution. In contrast to suggestions by Kondaurova *et al.*<sup>6</sup>, our model does not involve the Kelvin cascade but originates from the excitations created by a reconnection cusp. The distribution of Kelvin waves with different wavelengths, which becomes visible after the

cusp relaxes, can be understood to arise from the prereconnection dynamics where the minimum distance between vortices necessarily sweeps all length scales down to the core scale. Therefore, the cusp is built from Kelvin waves of different scale, limited only by the numerical resolution, that redistribute when the cusp relaxes.

Thus we conclude that the response to a single reconnection can take place without the excitation of a Kelvin-wave cascade. This statement was explicitly tested in vortex filament calculations for mutual friction dissipation down to  $\alpha \gtrsim 10^{-4}$  and additionally at  $T = 0$ . Instead the reconnection cusp leads to an exponential decay of the calculated rms curvature  $c_{\text{rms}}$  which can be associated with a Kelvin spectrum  $n(k) \propto k^{-\eta}$  in the range  $\eta \sim 3 \dots 3.5$ . We believe that this indicates that a universal Kelvin wave spectrum is not necessarily to be expected as a response to a single reconnection event.

## ACKNOWLEDGMENTS

This work was supported by the Academy of Finland (Grant No. 218211 and LTQ CoE grant). I am extremely grateful to M. Krusius for his comments and improvements for the paper. I also thank N. Hietala, V. L'vov, and W. Schoepe for their comments and suggestions and the CSC - IT Center for Science Ltd for the computational resources.

- 
- <sup>1</sup> B. V. Svistunov, Superfluid turbulence in the low-temperature limit, *Phys. Rev. B* **52**, 3647–3653 (1995).
  - <sup>2</sup> E. Kozik and B. Svistunov, Kelvin-Wave Cascade and Decay of Superfluid Turbulence, *Phys. Rev. Lett.* **92**, 035301 (2004).
  - <sup>3</sup> V. S. L'vov and S. Nazarenko, Spectrum of Kelvin-wave turbulence in superfluids, *JETP Lett.* **91**, 428–434 (2010).
  - <sup>4</sup> E. B. Sonin, Symmetry of Kelvin-wave dynamics and the Kelvin-wave cascade in the  $T = 0$  superfluid turbulence, *Phys. Rev. B* **85**, 104516 (2012).
  - <sup>5</sup> L. Boué, V. L'vov, and I. Procaccia, Temperature suppression of Kelvin-wave turbulence in superfluids, *Europhys. Lett.* **99**, 46003 (2012).
  - <sup>6</sup> L. Kondaurova, V. L'vov, A. Pomyalov, and I. Procaccia, Kelvin waves and the decay of quantum superfluid turbulence, *Phys. Rev. B* **90**, 094501 (2014).
  - <sup>7</sup> R. Hänninen, Dissipation enhancement from a single vortex reconnection in superfluid helium, *Phys. Rev. B* **88**, 054511 (2013).
  - <sup>8</sup> K. W. Schwarz, Three-dimensional vortex dynamics in superfluid <sup>4</sup>He: Line-line and line-boundary interactions, *Phys. Rev. B* **31**, 5782–5804 (1985).
  - <sup>9</sup> R. Hänninen and N. Hietala, Identification of Kelvin waves: numerical challenges, *J. Low Temp. Phys.* **171**, 485–496 (2013).
  - <sup>10</sup> W. F. Vinen and J. J. Niemela, Quantum turbulence, *J. Low Temp. Phys.* **128**, 167–231 (2002).
  - <sup>11</sup> L. Boué, D. Khomenko, V. S. L'vov, and I. Procaccia, Analytic Solution of the Approach of Quantum Vortices Towards Reconnection, *Phys. Rev. Lett.* **111**, 145302 (2013).
  - <sup>12</sup> S. Zuccher, M. Caldari, A. W. Baggaley, and C. F. Barenghi, Quantum vortex reconnections, *Phys. Fluids* **24**, 125108 (2012).
  - <sup>13</sup> S. Nazarenko, Kelvin wave turbulence generated by vortex reconnections, *JETP Lett.* **84**, 585–587 (2007).
  - <sup>14</sup> This estimation for the energy related to Kelvin waves is also consistent with Ref. [7], where the extra mutual friction dissipation originating from the reconnection was evaluated numerically.
  - <sup>15</sup> D. Kivotides, J. C. Vassilicos, D. C. Samuels, and C. F. Barenghi, Kelvin Waves Cascade in Superfluid Turbulence, *Phys. Rev. Lett.* **86**, 3080 (2001).
  - <sup>16</sup> A. W. Baggaley and C. F. Barenghi, Spectrum of turbulent Kelvin-waves cascade in superfluid helium, *Phys. Rev. B* **83**, 134509 (2011); in the related arXiv version one may observe that the Kelvin wave cascade (present in Fractalization and emission of vortex rings in the Kelvin waves cascade, [arXiv:1006.2934v1](https://arxiv.org/abs/1006.2934v1)) originating from single reconnection disappears as the numerics is improved (absent in Spectrum of turbulent Kelvin-waves cascade in superfluid helium, [arXiv:1006.2934v3](https://arxiv.org/abs/1006.2934v3)).